

Structural and electronic properties of Ge_nm^- and KGe_n^- Zintl anions ($n=3-10; m=2-4$) from density functional theory

Si-Dian Li, Qiao-Ling Guo, Xiu-Feng Zhao, Hai-Shun Wu, and Zhi-Hao Jin

Citation: *The Journal of Chemical Physics* **117**, 606 (2002); doi: 10.1063/1.1482068

View online: <http://dx.doi.org/10.1063/1.1482068>

View Table of Contents: <http://scitation.aip.org/content/aip/journal/jcp/117/2?ver=pdfcov>

Published by the [AIP Publishing](#)

Articles you may be interested in

An all-electron density functional theory study of the structure and properties of the neutral and singly charged M_{12} and M_{13} clusters: $\text{M} = \text{Sc-Zn}$

J. Chem. Phys. **138**, 164303 (2013); 10.1063/1.4799917

Stability of small Pd_n ($n = 1 - 7$) clusters on the basis of structural and electronic properties: A density functional approach

J. Chem. Phys. **127**, 244306 (2007); 10.1063/1.2806993

Electronic structures and spectroscopic properties of nitrido-osmium(VI) complexes with acetylide ligands [$\text{Os N}(\text{C C R})_4 - \text{R H}, \text{C H}_3$, and Ph] by density functional theory calculation

J. Chem. Phys. **124**, 144309 (2006); 10.1063/1.2189220

Spectroscopic properties of novel aromatic metal clusters: NaM_4 ($\text{M} = \text{Al, Ga, In}$) and their cations and anions

J. Chem. Phys. **120**, 10501 (2004); 10.1063/1.1738112

Photoelectron spectroscopy of copper cyanide cluster anions: On the possibility of linear and ring structures

J. Chem. Phys. **113**, 1725 (2000); 10.1063/1.481974



2014 Special Topics

PEROVSKITES

2D MATERIALS

MESOPOROUS MATERIALS

BIOMATERIALS/ BIOELECTRONICS

METAL-ORGANIC FRAMEWORK MATERIALS

AIP | APL Materials

Submit Today!

Structural and electronic properties of Ge_n^{m-} and KGe_n^- Zintl anions ($n=3-10; m=2-4$) from density functional theory

Si-Dian Li

Department of Chemistry, Xinzhou Teachers' University, Xinzhou 034000, Shanxi, People's Republic of China and School of Materials Science and Engineering, Xian Jiaotong University, Xian 710049, People's Republic of China

Qiao-Ling Guo and Xiu-Feng Zhao

Taiyuan Teachers' College, Taiyuan 030001, Shanxi, People's Republic of China

Hai-Shun Wu

Institute of Materials Chemistry, Shanxi Normal University, Linfen 041000, Shanxi, People's Republic of China

Zhi-Hao Jin

School of Materials Science and Engineering, Xian Jiaotong University, Xian 710049, People's Republic of China

(Received 21 December 2001; accepted 9 April 2002)

Structural optimizations and frequency analyses have been performed on free Ge_n^{m-} and KGe_n^- ($n=3-10, m=2-4$) Zintl anions and ionization potentials and electron affinities calculated for KGe_n using the density functional theory (DFT) of Becke's three-parameter hybrid functional with the Perdew/Wang 91 expression. The DFT results obtained for small clusters ($n=3-5$) are further checked with both the second-order Møller–Plesset perturbation theory (MP2) and the configuration interaction calculations with all single and double substitutions from the Hartree–Fock reference determinant (CISD). Free Ge_n^{2-} anions are found to share the same geometries as naked Zintl anions observed in solids with a systematical expansion in bond lengths within about 5%. Intensive searches indicate that two isomers, a tricapped trigonal prism (D_{3h}) and a slightly distorted tricapped trigonal prism (C_{2v}), exist for Ge_9^{2-} and Ge_9^{3-} , while *nido*- Ge_9^{4-} clearly favors the monocapped antisquare prism (C_{4v}) structure. HOMO-LUMO energy gaps >2.23 eV are obtained for Ge_n^{m-} series at the DFT level, except Ge_9^{3-} which has a much narrower energy gap of 1.16 eV. The calculated Gibbs free energy change of $\text{Ge}_9^{2-} + \text{Ge}_9^{4-} = 2 \text{ Ge}_9^{3-}$ conversion reaction involving nonagermanides has the value of $\Delta G^\circ = -2.91 \times 10^5 \text{ J mol}^{-1}$, providing the first quantum chemistry evidence that the geometrically deduced mixed valent couple of Ge_9^{2-} and Ge_9^{4-} in a previous study is thermodynamically unstable compared to two Ge_9^{3-} anions. The calculated stabilization energies of Ge_n^{2-} , Ge_n^- , and Ge_n exhibit similar variation trends, clearly indicating a maximum at $n=7$, a minimum at $n=8$, and an obvious recovery at $n=9$ and 10. The calculated normal vibrational frequencies reproduce the six observed Raman peaks of naked Ge_5^{2-} with an averaged discrepancy of 11 cm^{-1} . Face-capped or edge-capped deltahedral structures are predicted for binary KGe_n^- anions and KGe_n and K_2Ge_n neutrals. The magic numbers at $n=5, 9$, and 10 obtained in both stabilization energies and ionization potentials well reproduce the abundance distributions of KGe_n^- observed in time-of-flight mass spectra. The validity of the Zintl–Klemm–Busmann principle in KGe_n and K_2Ge_n neutrals is supported by the finding that sizable electron transfers from K atoms to Ge_n nuclei occur in these clusters and the Ge_n nuclei approach corresponding structures of free closo- Ge_n^{2-} anions. © 2002 American Institute of Physics. [DOI: 10.1063/1.1482068]

I. INTRODUCTION

The relationship between structures and stabilities of homoatomic E_n^{m-} and heteroatomic AE_n^- Zintl anions ($\text{E} = \text{Ge, Sn, Pb, A} = \text{K, Na, Cs, } n=3-10, \text{ and } m=1-4$) in condensed phases and that in gas phase has received considerable attention in the past two decades.¹⁻⁴ Ge_n -containing Zintl anions, which have the remarkable feature towards formation in solids, in solutions, and in gas phase, are of special interest for both fundamental and technological reasons. To date, the structurally characterized naked Ge_n^{m-} an-

ions in condensed phases include the distorted trigonal bipyramid Ge_5^{2-} ($\sim D_{3h}$),² distorted tricapped trigonal prism (TTP) Ge_9^{2-} ($\sim D_{3h}$ or $\sim C_{2v}$),³ distorted Ge_9^{3-} ($\sim C_{2v}$ or $\sim C_s$) between the boundaries of TTP and the monocapped antisquare prism (MASP),⁴⁻⁶ slightly distorted MASP Ge_9^{4-} ($\sim C_{4v}$),³ and the distorted bicapped antisquare prism (BASP) Ge_{10}^{2-} ($\sim D_{4d}$).⁴ Most of these naked Ge_n^{m-} anions exist as $[\text{A}([2,2,2]\text{crypt})]^+$ ($\text{A} = \text{K, Na}$) salts and have the actual site symmetry of C_1 . In these complexes, 2,2,2-crypt serves as complexing agent to encapsulate the alkali cations

and to provide channels big enough to accommodate Ge_n^{m-} anions. Ge_4^{2-} was first observed in $[\text{Na}([2,2,2]\text{crypt})]_2\text{Ge}_4$, but the attempt to determine its precise configuration failed because Ge_4^{2-} anions were found disordered in the crystal.⁷ The only octahedral Ge_6 unit with a D_4 symmetry obtained through another synthesizing route were identified in $[\text{Ge}_6\{\text{Cr}(\text{CO})_5\}_6]^{2-}$.⁸ There have been no experimental observations reported for Ge_7^{2-} and Ge_8^{2-} to date, showing the high instabilities of these two anions. It is interesting to note that Ge_9 anions was proposed to exist as the mixed valent system of Ge_9^{2-} and Ge_9^{4-} in $[\text{K}-(2,2,2)\text{-crypt}]_6 \cdot \text{Ge}_9\text{Ge}_9 \cdot (\text{en})_x$ ($x=2.5$).³ This charge assignment based on their geometrical relationship to Sn_9^{4-} (C_{4v}) and $\text{B}_9\text{H}_9^{2-}$ (D_{3h}) has been challenged by recent discovery of similar complexes $[\text{K}-(2,2,2)\text{-crypt}]_6 \cdot \text{Ge}_9\text{Ge}_9 \cdot (\text{en})_x$ ($x=0.5, 1.5$), in which the total negative charge of -6 was equally assigned to two well separated paramagnetic Ge_9^{3-} anions with slightly different shapes.⁶ Except for singly charged Ge_n^- , however, there have been no experimental observations reported in gas phase so far for highly charged Ge_n^{m-} with $m \geq 2$. Singly charged binary anions AGe_n^- ($A=\text{K}, \text{Na}, \text{Rb}, n=5-13$) were recently detected in TOF mass spectrometry by Fassler *et al.*¹ Magic numbers with high abundance at $n=5, 9$, and 10 , lower intensities at $n=11$ and 13 , and trace KGe_8^- were observed in recent TOF mass spectra, but clusters with $n=6$ and 7 and $n=2-4$ were completely absent. Applying the Zintl–Klemm–Busmann principle¹⁰ to these mixed anions, in other words, transferring the s electron from the more electropositive alkali metal atoms A to the Ge_n cluster nuclei, the doubly charged Ge_n^{2-} anions result. Metal atom face-capped or edge-capped structures are possible low-energy geometries for these binary anions and the Ge_n nuclei in them are expected to approach the geometries of naked Ge_n^{2-} . Unfortunately, the quantities of these cluster anions detected in gas phase are extremely small, making isolation and spectroscopic studies almost impossible at current stage.

Electronic calculations on germanium clusters have been limited to Ge_n neutrals and singly charged Ge_n^- and Ge_n^+ ions.^{11–15} They are found to be typical covalent systems following the prolate stack growth pattern of TTP Ge_9 subunits in medium-size range. DFT calculations have indicated that small Ge_n^- anions with $2n+1$ skeletal electrons (s.e.) favor the distorted structures of closo- Ge_n^{2-} (s.e. = $2n+2$) or nido- Ge_n^{4-} (s.e. = $2n+4$), i.e., a trigonal bipyramid for Ge_5^- (D_{3h}), a square bipyramid for Ge_6^- (D_{4h}), a pentagonal bipyramid for Ge_7^- (D_{5h}), a distorted face-capped pentagonal bipyramid for Ge_8^- (C_1 or $\sim C_s$), a distorted MASP for Ge_9^- (C_1 or $\sim C_{4v}$), and a slightly distorted BASP for Ge_{10}^- (C_1 or $\sim C_{4v}$).¹³ For highly charged Ge_n^{m-} with $m \geq 2$, quantum chemistry study has been limited to semiempirical extended Huckel molecular orbital (EHMO) calculations on Ge_9^{m-} ($m=2,3,4$) and Ge_{10}^{2-} .⁴

Having briefly reviewed the research works already performed on Ge_n -related clusters above, we think a proper understanding based on strict electronic calculations of Ge_n -containing Zintl anions will be necessary to fill the gap between theory and experiments. We present in this work a

systematic density functional theory investigation on Ge_n^{m-} and AGe_n^- anions and AGe_n and A_2Ge_n neutrals ($n=3-10$; $A=\text{K}, \text{Na}, \text{Rb}, \text{Cs}$). The DFT ground-state structures and stabilization energies, electron affinities, ionization potentials, and vibrational frequencies of corresponding systems are expected to serve as useful references for predicting or explaining future experimental observations of Ge_n -containing systems. We compare our optimized structures of free Ge_n^{m-} with that of naked Ge_n^{m-} observed in solids, predict structural and electronic properties for AGe_n^- anions and AGe_n and A_2Ge_n neutrals, and describe the extent of electron transfer from metal atoms A to the Ge_n nuclei. Naked Ge_n^{m-} are optimal systems for a detailed DFT study for two reasons: First, these anions are stable only when located in big channels created by special sequestering agents like $[2,2,2\text{-crypt}]$ which prevents electron transfer back to alkali cations from the Ge_n anionic nuclei and they are therefore as close to “gas phase” as one can possibly come in condensed phases, and second, most clusters studied here, except Ge_9^{3-} , have large HOMO-LUMO gaps and no unpaired electrons, making the single configuration ground-state calculations good approximations. This work is also a logical extension of our previous DFT studies on Ge_n and Ge_mSi_n microclusters,^{13,14} from neutrals and singly charged ions to highly charged anions and binary systems containing metal atoms.

II. METHODOLOGY

Structural optimizations in this work have been performed using the density functional theory of Becke’s three-parameter hybrid functional with the Perdew/Wang 91 expression (B3PW91). Frequency analyses at the optimized structures are carried out at the same theoretical level to clarify if the optimized structures are true minima or transition states on the potential energy surfaces of specific clusters. The choice of density functional method has been fully justified for Ge-containing systems for the reason that it is an *ab initio* tool and it includes the correlation effect which has been found necessary for germanium-related systems at relatively low computational cost.^{11,13,14} The initial structures of free Ge_n^{m-} are taken either from the results for singly charged Ge_n^- published before,^{11,13,15} or constructed according to the observed configurations in solids,^{2–8} or arbitrarily constructed to explore the configuration space more extensively. For binary clusters AGe_n^- , AGe_n , and A_2Ge_n ($A=\text{Li}, \text{Na}, \text{K}, \text{Rb}, \text{Cs}$), the metal atoms are initially arranged at face- or edge-capping positions with certain symmetry constraints. The initial structures are optimized with the basis of STO-3G first, and then fully optimized with the basis of 6-311G(d), which adds a single polarization function to 6-311G and results in one f function for first transition row atoms (d functions are already present for the valence electrons in these atoms), via the Berny algorithm in the GAUSSIAN ’98 code.¹⁶ The basis set used for AGe_n and A_2Ge_n neutrals with heavy alkali metals ($A=\text{Na}, \text{K}, \text{Rb}, \text{Cs}; n=5, 6$) was the Los Alamos National Laboratory sets (LanL) for effective core potential (ECP) of double- ξ type, namely, the LanL2DZ, which consists of a small core ECP with ns and np orbitals in the

valance space.¹⁶ Relativistic correlations for heavy atoms are considered in the ECP. Symmetry constraints are either reduced or removed whenever imaginary frequencies are found. For example, planar rhombus (D_{2h}), the ground-state structure for both the Ge_4 neutral and Ge_4^- anion,^{11,13} is found unstable for Ge_4^{2-} with an imaginary frequency at $84i \text{ cm}^{-1}$. The true ground-state structure of Ge_4^{2-} is found to be a butterfly (D_{2d}), which lies much lower in energy than both the rhombus and the tetrahedron (T_d). Concerning spin multiplicities, we choose singlet states for systems containing even number of electrons and doublet states for systems with odd number of electrons, considering the fact that only Ge_9^{3-} has been found paramagnetic in EPR experiments.⁴⁻⁶

The procedure outlined above has been successfully applied to small Ge_n neutrals, Ge_n^- and Ge_n^+ singly charged ions ($n \leq 10$), and semiconductor binary clusters A_nB_m ($A, B = \text{Si, Ge}; n + m \leq 10$).^{13,14} It is expected to produce reasonable results for Ge_n^{m-} anions ($m = 2, 3, 4$) and $A_l\text{Ge}_n$ ($l = 1, 2$) binary neutrals and anions in the same size range, for which strict electronic calculations have been lacking. Important low-energy structures at the DFT level are depicted in Fig. 1. These geometries have been confirmed to have no imaginary frequencies and therefore are true minima on potential energy surfaces of specific clusters. To check the effect of diffuse functions in basis sets, we compared the 6-311G(*d*) results shown in Fig. 1 with that of 6-311+G(*d*) basis which contains diffuse functions in the optimization processes for small naked anions ($n \leq 7$). Inclusion of diffuse functions in the basis sets turned out to have little influence on the optimized results at the DFT level. For example, the 6-311+G(*d*) bond lengths obtained for Ge_5^{2-} disagree with corresponding 6-311G(*d*) values only after the third decimals and both bases produce eventually the same vibrational frequencies as shown in Table II.

The DFT structures are further optimized employing the second-order Møller–Plesset perturbation theory (MP2) (Ref. 16) with the basis set of 6-311G(*d*) for Ge_n^{2-} in small size range ($n = 3-5$). The reoptimized geometries are found to be quite close to the DFT ones. For example, the DFT apical–equatorial (*a-e*) bond length r_{a-e} and equatorial–equatorial (*e-e*) bond length r_{e-e} for D_{3h} Ge_5^{2-} are 2.54 and 2.75 Å, respectively, close to corresponding MP2 values of 2.57 and 2.76 Å. The r_{a-e}/r_{e-e} ratio, which characterizes the D_{3h} geometry of Ge_5^{2-} , equals 0.92 at the DFT level and 0.93 at MP2. To clarify the proper level of basis sets and electron correlation of DFT and MP2 methods, configuration interaction calculations with all single and double substitutions from the Hartree–Fock reference determinant have also been performed for small clusters with the inclusion of all electrons (CISD(full)/6-31G).¹⁶ For Ge_5^{2-} at the CISD level, $r_{a-e} = 2.60$ and $r_{e-e} = 2.86$ Å, both slightly longer than corresponding DFT values, however, the bond length ratio $r_{a-e}/r_{e-e} \approx 0.91$ is kept almost the same as that of the DFT value of 0.92. The calculated results indicate that the geometrical shapes of the clusters checked are well maintained in these calculations though the structures may be expanded or compressed a little at different theoretical levels. The re-

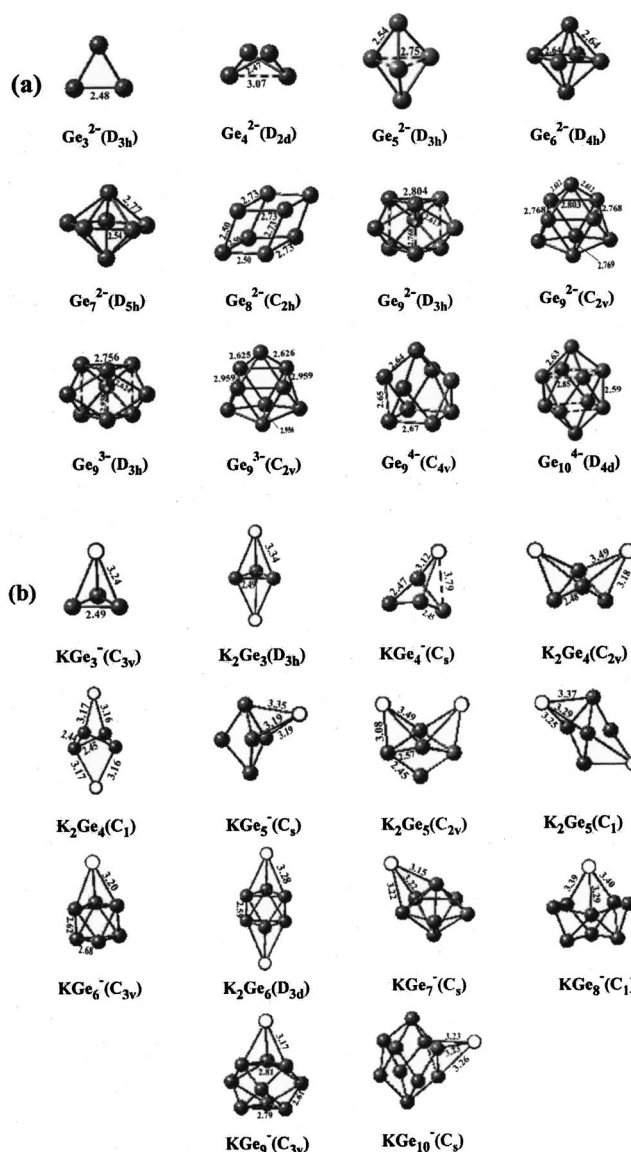


FIG. 1. Some of the low-energy structures of homoatomic Ge_n^{2-} anions (a) and singly-charged heteroatomic KGe_n^- anions and K_2Ge_n neutrals ($n = 3-10$) (b).

liability of DFT results obtained for bigger clusters are checked by comparison with available experimental results.

III. RESULTS AND DISCUSSIONS

A. Naked Zintl anions of the form Ge_n^{m-} ($n = 3-10, m = 2-4$)

closo- and nido-type structures are stable for Ge_n^{2-} with s.e. = $2n + 2$ and Ge_n^{4-} with s.e. = $2n + 4$, respectively, while Ge_n^- and Ge_n^{3-} systems with $2n + 1$ and $2n + 3$ skeletal electrons are expected to exist as variants between the two boundaries. To clarify this intuitive expectation, we optimize the ground-state structures (GSS) of Ge_n^{2-} , Ge_n^{3-} , and Ge_n^{4-} in this part first and compare them with available experimental results and DFT structures published before for Ge_n^- .^{11,13,15} Their calculated HOMO-LUMO energy gaps, stabilization energies, and the three strongest infrared vibrational frequencies are listed in Table I.

TABLE I. The lowest-energy structures, HOMO-LUMO gaps E_{gap} (eV), stabilization energies E_{stab} (eV/atom), and the three strongest infrared active vibration frequencies (cm^{-1}) of free Ge_n^{m-} anions obtained at the B3PW91-DFT/6-311G(d) level.

Ge_n^{m-}	Symmetry	State	E_{gap}	E_{stab}	The three strongest IR frequencies		
Ge_3^{2-}	D_{3h}	$^1A'_1$	2.63	1.85	199(E')		
Ge_4^{2-}	D_{2d}	1A_1	2.72	2.41	235(E)		
Ge_5^{2-}	D_{3h}	$^1A'_1$	3.56	2.86	260(A'_2)	196(A)	107(E')
Ge_6^{2-}	D_{4h}	$^1A_{1g}$	3.22	2.96	217(A_{2g})		
Ge_7^{2-}	D_{5h}	$^1A'_1$	2.88	3.05	182(A''_2)	222(E'_1)	
Ge_8^{2-}	C_{2h}	1A_g	2.34	3.02	259(B_u)	131(B_u)	61(A_u)
Ge_9^{2-}	C_{2v}	1A_1	2.23	3.21	149(A)	184(A_1)	103(B_1)
	D_{3h}	$^1A'_1$	2.23	3.21	148(E')	184(A)	103(E')
Ge_9^{3-}	D_{3h}	$^2A''_2$	1.16	2.65	223(E')	168(B)	192(A''_2)
	C_{2v}	2B_2	1.16	2.65	223(A)	168(A)	192(B_2)
Ge_9^{4-}	C_{4v}	1A_1	3.34	1.76	209(E)	217(A_1)	135(E)
Ge_{10}^{2-}	D_{4d}	1A_1	2.98	3.27	132(B_2)	224(B_2)	61(E_1)
	C_{2v}	1A_1	2.98	3.27	131(A_1)	223(A_1)	61(A)

Different from the Ge_3 neutral and Ge_3^- anion which have isosceles triangles (C_{2v}) as global minima, the GSS of Ge_3^{2-} is an equilateral triangle (D_{3h}) with a DFT bond length of 2.48 Å and a CISD bond length of 2.51 Å. Conflicting with both Ge_4 and Ge_4^- which have planar rhombus (D_{2h}) GSS, the optimized GSS of Ge_4^{2-} is a butterfly (D_{2d}) with the Ge–Ge bond length of 2.47 Å and Ge–Ge diagonal distance of 3.07 Å at the DFT level, while corresponding CISD values are 2.52 and 3.14 Å, respectively. This structure is 0.43 eV lower in energy than the planar rhombus (D_{2h}) which is confirmed to be a first-order stationary point with an imaginary frequency at $84i \text{ cm}^{-1}$ (B_{3g}). The trigonal pyramid Ge_4^{2-} (C_{3v}) is a local minimum 2.05 eV higher in energy than the butterfly global minimum. When triply charged, the GSS obtained for doublet Ge_4^{3-} remains as a butterfly. Further increasing the negative charge to -4 , a perfect tetrahedron (T_d) turned out to be the global minimum of Ge_4^{4-} with the bond length of 2.682 Å. It is easy to understand this structural evolution based upon the valence electron counts of these Ge_4 anionic units: Ge_4^{4-} has 20 s and p valence electrons to meet the requirement of $5n$ valence electrons for an electron-precise E_4 system and therefore favors the perfect tetrahedron structure (T_d), while Ge_4^- , Ge_4^{2-} , and Ge_4^{3-} belong to electron-deficiency systems and consequently possess structures with lower symmetries dis-

torted from the T_d tetrahedron. Fluxional behavior of Sn_4^{2-} in solution has been predicted⁹ and a similar situation is expected for Ge_4^{2-} . There have been no structural data from experiments for Ge_n^{2-} with $n \leq 4$ to compare with theoretical values.

Extensive calculations performed on closo- Ge_5^{2-} at various levels of theories are summarized in Table II. Its GSS is a trigonal bipyramid (D_{3h}), the same as that of Ge_5 and Ge_5^- . Remarkable is the increase of the apical–apical distance r_{a-a} with the increase of negative charges: r_{a-a} increases from 3.11 for Ge_5 , 3.63 for Ge_5^- to 3.96 Å for Ge_5^{2-} . The calculated $r_{a-e} = 2.54$ and $r_{e-e} = 2.75$ Å are about 0.06 Å longer than corresponding mean experimental values of 2.48 and 2.69 Å observed in (2,2,2-crypt-K⁺)₂. Ge_5^{2-} (where Ge_5^{2-} exists as a distorted trigonal bipyramid with the actual site symmetry of C_1),² but the bond length ratios are kept eventually the same in theory and experiment ($r_{a-e}/r_{e-e} \approx 0.92$), indicating that DFT Ge_5^{2-} is actually an expansion of its observed structure by about 2.4%. The strong bonding in the $a-e$ direction and weaker bonding in the $e-e$ direction are also confirmed by both the DFT Mulliken overlap population of $a-e/e-e = 0.3217/0.0889$ and the CISD value of 0.1508/−0.0793. In view of molecular orbital theory, the lowest unoccupied molecular orbital (LUMO) a''_2 of a Ge_5 neutral at the DFT level is characterized in the two apical atoms and filling extra electrons into this orbital increases the static repulsion in the direction of the three-fold axis. The calculated net charges on the two apical atoms increase from -0.09 for Ge_5 , -0.22 for Ge_5^- , and finally, to -0.44 for Ge_5^{2-} , leading to an increased static repulsion between the two apical atoms and therefore longer $a-a$ distances. Consequently, the r_{a-e}/r_{e-e} ratios for D_{3h} Ge_5^{m-} series increase steadily from 0.75, 0.85 to 0.92 with the increase of negative charges from $m=0, -1$, to -2 .

As expected from the electron counting rule, closo- Ge_6^{2-} has the square bipyramid (D_{4h}) as its GSS with the DFT bond length of $r_{a-e} \approx r_{e-e} = 2.64$ Å, about 0.11 Å longer than corresponding mean values of 2.54 and 2.52 Å observed in $D_4 [\text{Ge}_6\{\text{Cr}(\text{CO})_5\}_6]^{2-}$.⁸ Ge_6^{2-} shares the same geometry as Ge_6^- (though a little expanded) and has only one infrared active vibration mode (A_{2g}) located at 217 cm^{-1} . Similarly, Ge_7^{2-} possesses the pentagonal bipyramid (D_{5h} , $^1A'_1$) global minimum with $r_{a-e} = 2.77$ Å and $r_{e-e} = 2.54$ Å, again an elongated bipyramid structure (D_{5h}) compared to Ge_7 and

TABLE II. The apical–equatorial (r_{a-e}) and equatorial–equatorial (r_{e-e}) bond lengths (Å), the Mulliken overlap population ($\text{op}_{a-e}/\text{op}_{e-e}$), and normal vibration frequencies (cm^{-1}) of Ge_5^{2-} at different theoretical levels compared with corresponding experimental values for naked anions in solid (Ref. 2).

Method	r_{a-e}/r_{e-e}	$\text{op}_{a-e}/\text{op}_{e-e}$	Vibration frequency					
			A''_2	A'_1	E'	A'_1	E''	E'
Experiment	2.48/2.69			269		201	(190,185)	(111,91)
B3PW91/6-311G(d)	2.54/2.75	0.2518/0.0112	260	259	195	191	174	106
B2PW91/6-311+G(d)	2.54/2.75	0.1515/0.0563	260	259	194	188	173	106
B3PW91/6-311+G(3df,2p)	2.53/2.75	0.3217/0.0889	260	259	195	188	174	105
CISD(FC)/6-31G	2.60/2.87	0.1508/−0.079	244	246	190	193	157	106
CISD(FULL)/6-31G	2.60/2.86	0.1500/−0.081						
MP2/6-311G(d)	2.57/2.76	0.2918/−0.002						

Ge_7^- . The best structure we got for Ge_8^{2-} is a distorted biface capped octahedron (C_{2h}), similar to that of the C_{2h} Ge_8 neutral.¹³

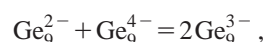
As mentioned in the Introduction, nonagermanide Ge_9^{m-} anions ($m=2,3,4$) have rich chemistries in solids and an unambiguous prove for the charge assignment of Ge_9^{2-} and Ge_9^{4-} is still in debate.⁶ This situation is simplified for free anions in gas phase. We have tried various kinds of initial structures for Ge_9^{2-} . The optimized results indicate that the regular TTP (D_{3h}) with the prism height of 2.768 Å has almost the same energy as a C_{2v} distorted MASP. The latter structure can also be viewed as a distorted TTP with one elongated prism height of 2.769 Å and two slightly shorter prism heights of 2.768 Å. The two structures produce eventually the same vibration frequencies as can be seen from Table I, further indicating that they are indistinguishable at the current DFT level. Similarly, Ge_9^{3-} , the only one paramagnetic anion with an unpaired electron, is found to have two isomers with almost the same energy—a regular TTP (D_{3h}) with the prism height of 2.958 Å and a distorted TTP (C_{2v}) which has one prism height of 2.956 Å and two slightly elongated prism heights of 2.959 Å. Ge_9^{4-} , a typical $2n+4$ system, clearly favors the C_{4v} MASP nido-type structure over a C_{2v} distorted MASP in total energy. The calculated bond lengths between capping atoms and the rectangular apical atoms are 2.61 Å in TTP Ge_9^{2-} , close to the averaged experimental value of 2.56 Å, while the DFT bond length of 2.80 Å in the triangular planes perpendicular to the threefold axis is 0.13 Å longer than the corresponding averaged experimental value of 2.67 Å.³ For Ge_9^{4-} , our optimized C_{4v} structure agrees well with its measured structure. For example, at the DFT level, $r_{a-e}=2.64$ and $r_{e-e'}=2.65$ Å, close to the averaged experimental values of 2.56 and 2.60 Å, respectively. There are several observed variants for Ge_9^{3-} in different salts.⁴⁻⁶ In our DFT C_{2v} Ge_9^{3-} , the three calculated prism heights are 2.956, 2.959, and 2.959 Å, respectively, qualitatively agreeing with the Ge_9^{3-} unit incorporated in $[\text{K-crypt}]_3\text{Ge}_9$ which has one shorter prism height of 2.868 Å and two elongated prism heights of 3.154 and 3.324 Å.⁵ The mean bond length in the triangles perpendicular to the threefold prism axis is 2.756 Å, about 0.10 Å longer than the averaged observed value of 2.657 Å.

The distorted bicapped antisquare prism structure ($\sim D_{4d}$) of decagermanide Ge_{10}^{2-} was resolved from a 1/3:2/3 disorder of the anions.⁴ Our calculated D_{4d} Ge_{10}^{2-} has an $a-e$ distance of 2.63 Å, an $e-e$ distance of 2.85 Å, and a bond length between $e-e'$ atoms in different planes of 2.59 Å, close to the corresponding averaged experimental values of 2.56, 2.85, and 2.52 Å, respectively. The relatively large bond length discrepancy between theory and experiment for Ge_{10}^{2-} is acceptable considering the fact that some of the interatomic distances could not be accurately determined in experiment due to the disorder of Ge_{10}^{2-} anions in solids.⁴

It is obvious from the discussion above that the optimized DFT Ge_n^{m-} free anions possess geometries in agreement with that of the naked Ge_n^{m-} anions observed in experiments and have longer bond lengths within about 5% than their counterparts incorporated in solids in most cases. MP2 and CISD bond lengths are found systematically longer than

corresponding DFT values as can be seen in the example of Ge_5^{2-} listed in Table II. With the CISD(FC)/6-31+G(*d*) method which contains diffuse functions in the basis, the optimized bond lengths obtained for Ge_3^{2-} and Ge_4^{2-} are 2.478 and 2.465 Å, respectively, very close to the DFT values shown in Fig. 1. We conclude that the theoretically optimized structures of free Ge_n^{m-} are eventually expansions of corresponding naked anions incorporated in solids and better agreement can be achieved by systematically scaling the theoretical structures. Concerning the long standing controversy about the instability of anions within DFT, we think that, the agreement of our DFT minima with that of more strict MP2 and CISD methods for small Ge_n anions ($n \leq 5$), and, more importantly, with available structures observed in solids in the size range of $n=5-10$, has provided strong supportive evidence for the stabilities of our DFT minima. In addition, it is unlikely that artifacts of the finite size of the basis sets within DFT can produce a systematical agreement as that achieved in this work.

To clarify the controversy over the proposal that independent Ge_9^{2-} and Ge_9^{4-} coexist in one crystal unit,³ we consider the energy balance in the following reaction:



where at the DFT level with the inclusion of zero-point correction, $\Delta E^\circ = -293$, $\Delta H^\circ = -293$, and $\Delta G^\circ = -291$ kJ mol⁻¹. The huge negative values of ΔE° , ΔH° , and ΔG° clearly indicate that, when two independent Ge_9 anions with a total charge of -6 coexist in one system, there would be a strong tendency to form two Ge_9^{3-} anions instead of the mixed valent couple of Ge_9^{2-} and Ge_9^{4-} . As an oxidizing agent, Ge_9^{2-} would be very unstable to coexist with a strong reducing agent Ge_9^{4-} . Similar conversion is expected to exist in condensed phases. If Ge_9^{2-} and Ge_9^{4-} coexisted in one structural unit, there would be an effective electron transfer between them, resulting in two Ge_9^{3-} anions. So our calculation provides the first quantum chemistry evidence that the mixed valent couple of Ge_9^{2-} and Ge_9^{4-} proposed for crystal $[\text{K}-(2,2,2)\text{-crypt}]_6\text{Ge}_9\text{Ge}_9(\text{en})_x$ ($x=2.5$) may have been converted into two Ge_9^{3-} anions automatically under equilibrium condition. In addition, it is hard to explain in experiments why $[\text{K}-(2,2,2)\text{-crypt}]_6\text{Ge}_9\text{Ge}_9(\text{en})_x$ ($x=0.5$ and 1.5) complexes consist of two separated paramagnetic Ge_9^{3-} anions confirmed by EPR measurements, while $[\text{K}-(2,2,2)\text{-crypt}]_6\text{Ge}_9\text{Ge}_9(\text{en})_{2.5}$, which differs from the former two only in the numbers of solvent molecules, possesses a charge disproportionation of Ge_9^{2-} and Ge_9^{4-} . Ge_9^{3-} anions are strongly favored in energy over the mixed valent system of Ge_9^{2-} and Ge_9^{4-} and the solvent effect is very unlikely to reverse this conversion reaction. The two well-separated naked Ge_9 anionic units in one crystal may well be two Ge_9^{3-} anions with different shapes rather than carrying different charges. For the same reason, it is expected that all the Ge_9 anions in different complexes labeled as 1a, 1b, 2a, 2b, and 2c in Ref. 6 are Ge_9^{3-} anions with slightly different shapes. Various evidences discussed above indicate that the structures of Ge_n^{m-} anions can not be expected to be rigid in condensed phases and very likely the relatively large Ge_9^{3-} anions behavior fluxionally in condensed phases, similar to

TABLE III. The optimized ground-state symmetries, stabilization energies E_{stab} (eV/particle), HOMO-LUMO energy gaps E_{gap} (eV), and the Mulliken charges on K atoms (PCs) of KGe_n^- , and the vertical ionization potentials VIPs (eV), the energies of HOMO orbitals E_{HOMO} (eV), and adiabatic electron affinities AEAs (eV) of KGe_n ($n=3-10$).

KGe_n	Symmetry	E_{stab}	Charges on	E_{gap}	E_{HOMO}	VIPs	AEAs
3	C_{3v}	2.98	+0.362	1.01	4.26	6.34	1.13
4	C_s	2.88	+0.467	1.47	4.51	6.22	1.51
5	C_s	3.81	+0.497	1.89	4.87	6.58	1.90
6	C_{3v}	3.16	+0.587	1.65	4.57	6.39	2.00
7	C_s	2.85	+0.642	1.48	4.07	5.58	1.57
8	C_1	3.70	+0.583	2.34	4.68	6.06	2.17
9	C_{3v}	4.25	+0.717	1.95	4.88	6.33	3.28
10	C_s	3.94	+0.692	2.33	5.01	6.35	2.64

butterfly K_2Ge_4 with the symmetry of C_1 results, which is 0.26 eV lower than the C_{2v} bi-face capped butterfly structure in energy. The D_{2d} bi-edge capped butterfly K_2Ge_4 isomer, which appears very similar to the C_1 structure in shape with four equal K-Ge bond lengths of 3.16 Å, lies only 0.00036 eV higher than the C_1 global minimum at the DFT level. The C_1 K_2Ge_4 possesses the positive charges of +0.723 on K atoms and the K-Ge distances between 3.16 and 3.17 Å. The butterfly Ge_4 nucleus is maintained with the averaged Ge-Ge bond length of 2.45 Å and the diagonal distance of 3.16 Å, close to corresponding values in the free butterfly Ge_4^{2-} .

KGe_5^- turned out to be a face-capped trigonal bipyramid ($C_s, ^1A'$) lying 0.018 eV lower in energy than the edge-capped trigonal bipyramid structure (C_{2v}). When two K atoms are capped on nonadjacent faces of a trigonal bipyramid Ge_5 , a distorted bicapped trigonal bipyramid K_2Ge_5 (C_1) results. This structure is 0.388 eV more stable than the adjacent bi-face capped C_{2v} screw K_2Ge_5 due to the weaker static repulsion between the capping K atoms existing in it. The two K atoms in C_1 K_2Ge_5 possess the positive charges of +0.716. This obvious electron transfer causes the Ge_5 nucleus to approach the s.e. = $2n+2$ requirement. In the Ge_5 nucleus in C_1 K_2Ge_5 , $r_{a-a} = 4.01$ Å and the averaged $r_{e-e} = 2.71$ Å, are both quite close to corresponding values of 3.96 and 2.75 Å in free D_{3h} Ge_5^{2-} .

Introducing a K atom to Ge_6^- produces a face-capped octahedron KGe_6^- ($C_{3v}, ^1A_1$) with the K-Ge bond length of 3.20 Å and the positive charge of +0.587 on the K atom. With one more K atom added on the opposite face, the bi-capped antitrigonal prism K_2Ge_6 ($D_{3d}, ^1A_{1g}$) results with the K-Ge bond length of 3.28 Å and the positive charge of +0.731 on both K atoms. KGe_7^- is a face-capped pentagonal bipyramid (C_s) with the averaged K-Ge bond length of 3.20 Å and a positive charge of +0.641 on K.

It is easy to conclude from above discussion that Ge_n nuclei in K_2Ge_n neutrals approach the $2n+2$ closo- Ge_n^{2-} deltahedral geometries as consequences of effective electron transfers from K atoms to Ge_n nuclei. This conclusion shows that the ZKB principle is applicable to small A_2Ge_n , paralleling the situation found in Sb_3SnA and Sb_3InA_2 in an *ab initio* study,¹⁰ where alkali atoms A function as electron donors and the Sb_3Sn and Sb_3In units approach the electron-

precise Sb_4 tetrahedron geometry with 20 valence electrons.

Structural optimization of KGe_n^- with $n \geq 8$ proves to be much more complicated and time consuming. A distorted face-capped antisquare prism KGe_8^- ($C_{2v}, ^1A_1$) is confirmed to have an imaginary frequency at $148i$ cm^{-1} . When the symmetry constraint is released, the lowest-energy structure obtained for KGe_8^- through a full structural optimization is a distorted tricapped antitrigonal prism with C_1 symmetry, lying 1.05 eV lower in energy than the C_{2v} one and possesses the positive charge of +0.585 on the K atom. KGe_9^- has a tetracapped TTP global minimum ($C_{3v}, ^1A_1$) with the K-Ge distance of 3.17 Å and the positive charge of +0.717 on K, but KGe_9 neutral failed to converge with this geometry during structural optimization. The best structure obtained for KGe_9 is a slightly distorted bi-face capped antisquare prism ($C_{2v}, ^2B_2$). Adding one face-capping K atom to the D_{4d} BASP Ge_{10}^- produces a face-capped distorted BASP KGe_{10}^- ($C_s, ^1A'$) with the averaged K-Ge bond length of 3.24 Å and the positive charge of +0.692 on the K atom. KGe_{10} neutral has a similar optimum structure ($C_s, ^2A'$). The C_s KGe_{10}^- is confirmed to be about 0.84 eV lower in energy than the pentacapped trigonal prism KGe_{10}^- ($C_{3v}, ^1A_1$) formed by adding a face-capping K atom on the tetracapped trigonal prism Ge_{10}^- (C_{3v}) along the threefold axis. It should be noted that KGe_{10}^- has higher stabilization energy than KGe_{10} , a stability order different from that of homoatomic Ge_n^{m-} ($m=0,1,2$), where decagermanides are more stable than nonagermanides (see Fig. 3).

As discussed above, KGe_n^- anions and KGe_n neutrals exist as face-capped or edge-capped deltahedral structures which are derivatives of corresponding Ge_n units in most cases. Their stabilization energies relative to independent Ge_n neutrals¹³ and K atoms are plotted in Fig. 4. Prominent maxima at $n=5$ and 9 and the high stabilization energies at $n=10$ and 8 clearly indicate that KGe_5^- , KGe_9^- , KGe_{10}^- , and KGe_8^- are the most stable species in this size range, while KGe_4^- and KGe_7^- exist as two local minima. This finding is in good accordance with the TOF mass spectrum of KGe_n^- in a laser desorption experiment of K_4Ge_9 alloy, where magic numbers were observed for KGe_5^- , KGe_9^- , and KGe_{10}^- with high abundances and a weak peak detected for KGe_8^- , while KGe_3^- , KGe_4^- , KGe_6^- , and KGe_7^- were absent completely.¹

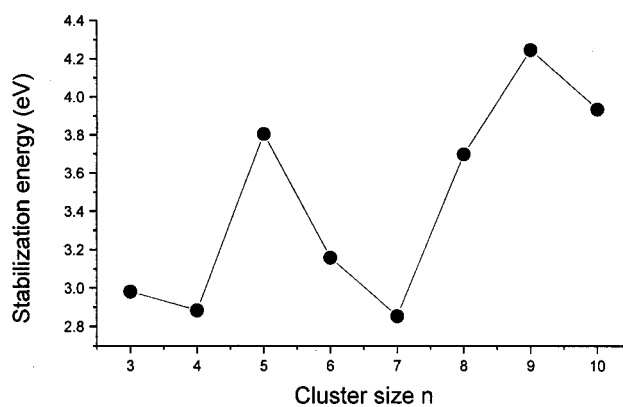


FIG. 4. Stabilization energies of singly-charged binary KGe_n^- anions ($n=3-10$).

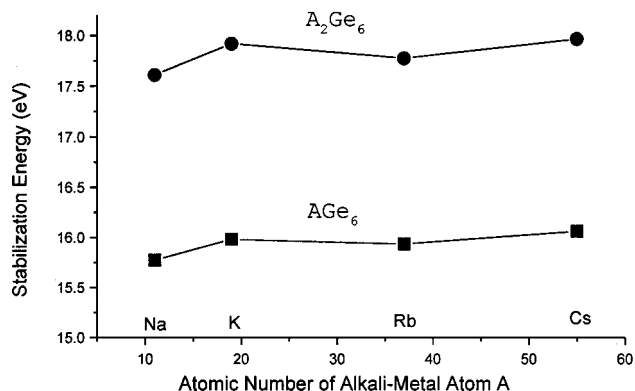


FIG. 5. Stabilization energies of binary AGe_6 (C_{3v}) and A_2Ge_6 (D_{3d}) neutrals with different alkali metals ($A=\text{Na}, \text{K}, \text{Rb},$ and Cs).

To investigate the relative stabilities of AGe_n and A_2Ge_n neutrals with different alkali atoms capped on the same Ge_n nuclei, the DFT stabilization energies of C_{3v} AGe_6 and D_{3d} A_2Ge_6 ($A=\text{Na}, \text{K}, \text{Rb}, \text{Cs}$) are shown in Fig. 5, using the basis set of LanL2DZ. Higher stabilities are found for $A=\text{K}$, and Cs where electron transfers occur most efficiently. Similar results are obtained for AGe_5 and A_2Ge_5 for which the highest stabilization energies also occur at $A=\text{K}$. This conclusion agrees with that drawn from an *ab initio* study on Sb_3SnA by Hagelberg *et al.*¹⁰

Using Koopman's theorem, energy of the HOMO E_{HOMO} can be used to estimate the ionization potential of AGe_n at first approximation. Vertical ionization potentials (VIPs) calculated as the energy difference between the optimum KGe_n neutrals and corresponding KGe_n^+ cations with the neutral geometries are tabulated and compared with E_{HOMO} in Table III and Fig. 6. The adiabatic electron affinities (AEAs) of KGe_n obtained as the energy difference between optimum KGe_n^- and KGe_n are also listed. VIP and E_{HOMO} vary with approximately the same trend as that of the stabilization energies of KGe_n^- displayed in Fig. 4; VIP and E_{HOMO} exhibit a maximum at $n=5$, an obvious recovery at $n=9$ and 10, and a clear minimum at $n=7$, again in agreement with the magic numbers observed for KGe_n^- in TOF mass spectroscopy.

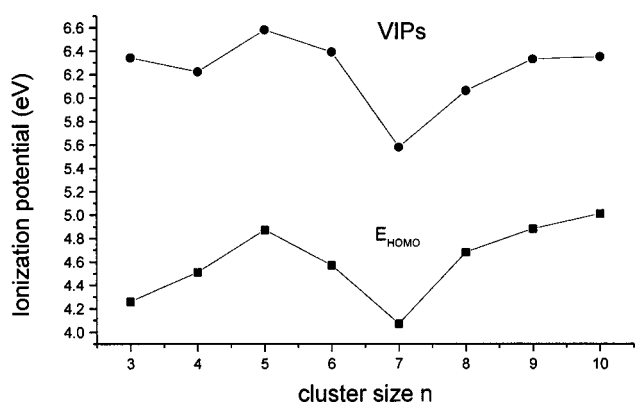


FIG. 6. The vertical ionization potentials (VIPs) and HOMO energies of corresponding KGe_n neutrals ($n=3-10$).

C. Normal vibration frequencies of closo- Ge_5^{2-}

Ge_5^{2-} is the only one species in the naked Ge_n^{2-} series which has experimentally known Raman spectra first compared and assigned by analogy with that of Bi_5^{3+} .^{2,19} Our calculated normal vibration frequencies for Ge_5^{2-} at different theoretical levels are compared with the measured Raman peak positions² in Table II. Of the 6 vibration bands $A_2'' + A_1' + E' + A_1' + E'' + E'$ of D_{3h} Ge_5^{2-} (corresponding to 9 vibrating modes), three $A_2'' + E' + E'$ are infrared active with the relative intensities of 1.000, 0.131, and 0.026, respectively, and five $A_1' + A_1' + E'' + E' + E'$ Raman active. The strongest band ν_1 at 269 cm^{-1} is assigned to the totally symmetric stretching mode A_1' , the second strongest band ν_2 at 201 cm^{-1} to the totally symmetrical stretching mode A_1' which mainly involves the stretching of the two apical atoms, and the third band ν_3 split into two peaks at 190 and 185 cm^{-1} assigned to the degenerate E'' mode, which has been split into two absorption peaks due to the symmetry reduction from D_{3h} adopted in calculation to C_1 at the real crystal site.² The two weakest broad bands ν_4 at 111 cm^{-1} and ν_5 at 91 cm^{-1} are attributed to the degenerate band E' , which is both Raman and infrared active and has been split into two normal vibrational modes with all atoms vibrating in the directions perpendicular to the threefold axis. Failure to observe the two Raman forbidden bands A_2'' and E' located at 260 and 195 cm^{-1} at the DFT level, which are the two most intensive infrared bands, indicates that vibration coupling at the C_1 crystal site is not significant, as noticed in Ref. 2. An averaged discrepancy of 11 cm^{-1} between the six measured Raman peaks and the calculated Raman allowed bands at the DFT level is satisfactory, considering the fact that the calculated DFT frequencies are for the free D_{3h} Ge_5^{2-} anion and large uncertainties existed in experiments in determining the exact locations of the weak and broad Raman bands, especially ν_4 and ν_5 .² The largest discrepancy of 15 cm^{-1} does occur at ν_5 which belongs to the degenerate E' energy band split due to the symmetry reduction in the real crystal.

IV. SUMMARY

We have performed a systematical DFT investigation on highly charged Ge_n^{m-} ($m=2, 3, 4, n=3-10$), singly charged KGe_n^- , and neutral K_2Ge_n in this work. Homatomic free Ge_n^{m-} anions are found to follow the closo-type structures for singly, doubly, and triply charged anions ($m=1,2,3$), while the quadruply charged Ge_9^{4-} favors a nido-type C_{4v} structure. Stabilization energies of Ge_n , Ge_n^- , and Ge_n^{2-} exhibit a quick increase from $n=4$ to $n=5$, a clear maximum at $n=7$, and an obvious recovery at $n=9$ and 10, while the Ge_8 units exist constantly as local minima in all three cases. As an example, a DFT assignment of the six observed Raman peaks of Ge_5^{2-} with a discrepancy of 11 cm^{-1} is presented. The controversy over the charge dislocation of Ge_9^{2-} and Ge_9^{4-} is discussed in detail. Our DFT calculation suggests that the $\text{Ge}_9^{2-} + \text{Ge}_9^{4-}$ mixed valent ionic couple be automatically converted into two Ge_9^{3-} anions for

thermodynamic reasons. Face-capped or edge-capped delta-hedral structures are predicted for KGe_n^- anions and KGe_n and K_2Ge_n neutrals. Stabilization energies of KGe_n^- anions exhibit two maxima at $n=5$ and 9, high stabilities at $n=8$ and 10, and two minima at $n=4$ and 7. VIPs and E_{HOMO} of KGe_n are found to follow approximately the same variation trend as that of the stabilization energies. The theoretically obtained magic numbers at $n=5, 9$ and 10 agree well with the abundance distributions of KGe_n^- observed in TOF mass spectra.

Medium-sized Ge clusters containing several dozens of atoms have been detected in gas phase²⁰ and discrete large Ge_n^{m-} clusters predicted to exist in solids and solution.¹ It still remains a huge challenge in both theory and experiments to explore the structural relationship between them in different phases and to describe the structural transition from prolate stacks to the bulklike spheres as cluster sizes increase. Further more, transition metal-containing CoGe_n^- anions which contain the triply charged Ge_n^{3-} nuclei, were recently discovered in gas phase with the magic number of $n=9$ and 10.²¹ This discovery presents an interesting topic in theory to compare structures and properties of MGe_n^- with that of AGe_n^- clusters studied in this work.

- ¹T. F. Fassler, H. J. Muhr, and M. Hunziker, *Eur. J. Inorg. Chem.* **1998**, 1433.
- ²J. Campbell and G. J. Schrobilgen, *Inorg. Chem.* **36**, 4078 (1997).
- ³C. H. E. Belin, J. D. Corbett, and A. Cisar, *J. Am. Chem. Soc.* **99**, 7163 (1977).
- ⁴C. Belin, H. Mercier, and V. Angilella, *New J. Chem.* **15**, 931 (1991).
- ⁵T. F. Fassler and M. Hunziker, *Inorg. Chem.* **33**, 5380 (1994).
- ⁶T. F. Fassler and U. Schutz, *Inorg. Chem.* **38**, 1866 (1999).
- ⁷S. C. Critchlow and J. D. Corbett, *J. Chem. Soc. Chem. Commun.* **1981**, 236.
- ⁸P. Kirchner, G. Huttner, K. Heinze, and G. Renner, *Angew. Chem. Int. Ed. Engl.* **37**, 1664 (1998).
- ⁹M. J. Rothman, L. S. Bartell, and L. L. Lohr, *J. Am. Chem. Soc.* **103**, 2482 (1981).
- ¹⁰F. Hagelberg, S. Srinivas, N. Sahoo, and T. P. Das, *Phys. Rev. A* **53**, 353 (1996).
- ¹¹E. F. Archibong and A. St-Amant, *J. Chem. Phys.* **109**, 962 (1998).
- ¹²J. Wang, G. Wang, and J. Zhao, *Phys. Rev. B* **64**, 205411 (2001).
- ¹³Si-Dian Li, Z. G. Zhao, H. S. Wu, and Z. H. Jin, *J. Chem. Phys.* **115**, 9255 (2001).
- ¹⁴Si-Dian Li, Z. G. Zhao, X. F. Zhao, H. S. Wu, and Z. H. Jin, *Phys. Rev. B* **64**, 195312 (2001).
- ¹⁵P. W. Deutsch, L. A. Curtiss, and J.-P. Blaudeau, *Chem. Phys. Lett.* **344**, 101 (2001).
- ¹⁶M. J. Frisch *et al.*, GAUSSIAN 98, Revision A.6, Gaussian, Inc., Pittsburgh, PA, 1998.
- ¹⁷R. W. Rudolph and W. L. Wilson, *J. Am. Chem. Soc.* **103**, 2480 (1981).
- ¹⁸J. M. Hunter, J. L. Fye, and M. F. Jarrod, *Phys. Rev. Lett.* **73**, 2063 (1994).
- ¹⁹S. Ulvenlund, K. Stahl, and L. Bengtsson-Kloo, *Inorg. Chem.* **35**, 223 (1996).
- ²⁰A. A. Shvartsburg and M. F. Jarrod, *Phys. Rev. A* **60**, 1235 (1999).
- ²¹X. Zhang, G. Li, and Z. Gao, *Rapid Commun. Mass Spectrom.* **15**, 1573 (2001).